

## A robust multi-image phase retrieval



Cheng Guo<sup>a</sup>, Cheng Shen<sup>a</sup>, Jiubin Tan<sup>a</sup>, Xuejing Bao<sup>a</sup>, Shutian Liu<sup>b</sup>, Zhengjun Liu<sup>a,\*</sup>

<sup>a</sup> Department of Automatic Test and Control, Harbin Institute of Technology, Harbin 150001, China

<sup>b</sup> Department of physics, Harbin Institute of Technology, Harbin 150001, China

### ARTICLE INFO

**Keywords:**  
Phase retrieval  
Diffraction

### ABSTRACT

The phase evaluation is not perfect by using three kinds of existing multi-image phase retrieval methods. The amplitude-phase retrieval scheme is employed for initializing the input of the Multi-stage algorithm to obtain a robust result. The synthesized axial multi-image phase retrieval technique is able to be highly accurate convergent with continuous phase distribution of  $[0, 2\pi]$  and random phase distribution of  $[0, \pi]$ , which is also demonstrated to have sharper edge for reconstructed phase map in experiment. This paper will provide a powerful and useful guidance for axial multi-image phase retrieval.

© 2017 Elsevier Ltd. All rights reserved.

### 1. Introduction

Iterative phase retrieval has been a powerful tool to reconstruct the complex amplitude of sample by the back-and-forth beam propagation between the measuring plane and the sample plane with the addition of different constraints. To date, iterative phase retrieval technique has been successfully applied in encryption [1,2], electron microscopy [3], quantum imaging [4], super-resolution imaging [5]. As the origin of iterative phase retrieval algorithm, Gerchberg-Saxton (GS) algorithm [6] reconstructs the phase of sample with a pair of known amplitude distribution at the sample plane and the measuring plane. Its low convergence speed and much sensitivity to the initial value, however, restrict its application. Moreover, another limitation of GS algorithm lies on that the amplitude distribution of sample has to be determined, which usually imposes more complexity in experimental setup. Thus, based on the origin, hybrid input output (HIO) algorithm [7] was brought up by using the support constraint to increase the convergence speed. In spite of higher convergence speed and high precision, both algorithms require that the support constraint should be tight.

To overcome these limitations, multi-image phase retrieval algorithms have been proposed [8–18] afterwards. They introduce variable optical system parameters to generate multiple measurements and get rid of the prior knowledge of amplitude distribution at the sample plane. The methodology can be divided into two categories: lateral and axial scanning strategies. As a lateral scanning technique, the ptychographic iterative engine (PIE) algorithm [8] shifts an aperture or a pinhole to create a series of overlapped diffraction patterns at the measuring plane. Its demanding shifting operation slows down the reconstruction and leads to a long acquisition time, which is then improved by LED array mi-

croscope [9], parallel calculation [10], and modulation imaging with a measured loose support [11]. Recently, these lateral scanning methods, such as single-shot ptychography [12] and Fourier ptychographic microscopy [5], have made lots of achievements theoretically and experimentally. For axial scanning, the single-beam, multiple-intensity reconstruction technique (SBMIR) algorithm [13] and the multi-stage algorithm [14] both sequentially record diffraction and then process them serially in the iterative update. By contrast, the amplitude-phase retrieval (APR) algorithm [15] deals with the measured diffraction patterns in a parallel way and averages the estimations in the real space. It has been demonstrated by experiment that these axial scanning algorithms can be realized by using focus tunable lens [16], multiple wavelengths [17], and multiple measuring distances [18].

Currently, all researches about these axial methods pay more attention on retrieving the object amplitude than the phase. But phase usually reflects much intrinsic information on the sample, for example, the thickness of transparent biological specimens. Also, the discussion of these methods does not cover the application range where the object size varies. Due to the two reasons, this paper investigates the performance of three axial multi-image phase retrieval algorithms, including SBMIR, Multi-stage and APR algorithm, under two typical object phase distributions. Then, we discover their respective disadvantages. To tackle the issue, we propose a new hybrid algorithm, which achieves robust phase reconstruction while keeping a high-precision amplitude retrieval and significantly reduces sensibility to the initialization. Also, we define the dynamic range where these axial methods can effectively work, which distinguishes them from the lateral scanning techniques. Thus, it will be an instructive guideline for applying these popular algorithms. At length, the performance of our hybrid approach is also demonstrated in experiment.

\* Corresponding author.

E-mail address: [zjliu@hit.edu.cn](mailto:zjliu@hit.edu.cn) (Z. Liu).

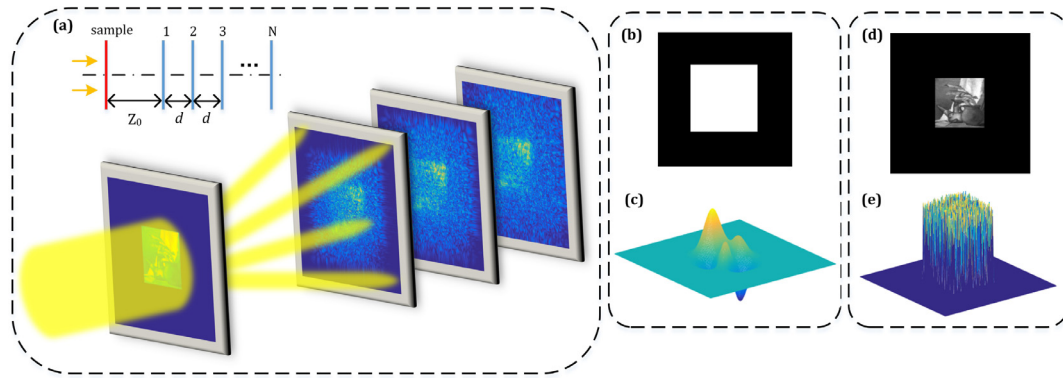


Fig. 1. Schematic diagram of axial multi-image phase retrieval experiment (a) and tested samples for simulation: the multiplication of (b) and (c) forms an ideal complex amplitude function with a continuous phase; (d) and (e) forms one with a random phase. Both of them are rasterized in  $256 \times 256$  pixels.

## 2. Reconstructed performance analysis

Before the further analysis, the optical system parameters need to be declared. The total of intensity measurements  $N$  is 8. Here the angular spectrum analysis method is utilized to depict the free-space propagation in Fig. 1(a). To satisfy the sampling theorem in simulation, the pixel number of image  $M \times M$ , the physical side length  $L$ , the working wavelength  $\lambda$  and the diffraction distance  $Z$  should follow [19]

$$Z^2 \geq \frac{L^4}{M^2 \lambda^2} - L^2. \quad (1)$$

Besides, it can be easily proved that once the first diffraction distance  $Z_0$  meets the sampling condition, the sequential distances  $Z = Z_0 + (n-1)d$ ,  $1 \leq n \leq N$  comply with it as well.

Fig. 1(c) and (e) are two typical sample phase distributions, namely the continuous one and the random one. The former denotes the condition that the wave front gives a global smooth change and there are no singular points in the 2-D distribution. By contrast, the latter is generated from the normal Gaussian distribution, representing the condition with manifold jumps. Combined with a square pupil in Fig. 1(b) and a still object sketch picture in Fig. 1(d) [20] as the amplitude function separately, they form a pair of tested complex amplitude functions, which are taken as the ground truth for the following simulations.

Generally, the mean square error (MSE) between the reconstructed and true amplitude distribution is adopted as an indicator of recovery accuracy. In this paper, we utilize the modified version of this metric to clarify the retrieved quality for amplitude and it is defined as

$$\text{LMSE} = \log_{10} \left( \frac{1}{M \times N} \sum_{m,n} ||A_{est}| - |A_0||^2 \right), \quad (2)$$

where  $A_{est}$  and  $A_0$  denote the reconstructed amplitude and the object amplitude respectively. For the phase, we bring standard deviation for phase convergence criterion like as [13]

$$\text{LSTD} = \log_{10} [\text{std}(\varphi_{est} - \varphi_0)], \quad (3)$$

where the symbol “std” denotes the standard deviation between the estimated phase  $\varphi_{est}$  and the true phase  $\varphi_0$ .

When the continuous phase ranges from  $-\pi$  to  $\pi$  and the random phase from 0 to  $\pi$ , the LSTDs of these three axial algorithms are pictured in Fig. 2 as the intensity measurements are taken at different positions in the diffraction field of object. To denote the displacement, the first diffraction distance  $Z_0$  increases from 15 mm to 110 mm with an interval of 5 mm. The distance  $d$  between two consecutive measuring planes follows the same value variation as  $Z_0$  does. The working wavelength is 632.8 nm. The initialization of these three methods is set as a zero matrix and the iterative procedure is executed until 1000 times in all simulations. With these assumptions, the recovery performance of whole diffraction field is able to be built in Fig. 2. Especially, each pair of  $(Z_0, d)$  represents one of reconstructed results in the diffraction field.

As is shown in Fig. 2 (a)–(c), three axial algorithms behave differently for the recovery of object with a continuous phase. Two serial computing algorithms, SBMIR and Multi-stage, can obtain an excellent phase reconstruction wherever the measurements are in the diffraction field. However, the retrieved result from APR, the parallel multi-image algorithm, has a high LSTD from the ground truth overall, and even appears a failure at some peculiar measurement conditions.

It is the converse for the random phase condition. Almost all measurements from the whole diffractive field guarantee an accurate phase reconstruction for APR, whose LSTD keeps around  $-20$  orders of magnitude in Fig. 2(e). Nevertheless, the error distributions from SBMIR algorithm and Multi-stage algorithm are quite wavy and fluctuate heavily at some particular pairs  $(Z_0, d)$  values shown in Fig. 2(d) and (f). This means that these two serial calculation strategies are sensitive to the position of measuring planes in the diffraction field. Once  $Z_0$  is chosen improperly, they will converge to a wrong solution.

To conclude, neither of the serial and parallel multi-image algorithms are able to have stable excellent performance to retrieve different forms of phase. Usually, phase information reveals the variation of sample thickness or refractivity. Continuous phase distribution represents a low gradient variation of the index while random phase distribution belongs a high one. Considering that the observed sample is complicated in reality, it is nearly impossible to predict the phase form ahead. Therefore, both serial and parallel calculating methods could be impotent. Also, the sample phase distribution may behave a mixture of the continuous and random ones. An ambidextrous algorithm is needed to tackle the phase issue.

## 3. Hybrid approach

Here, we put forward a hybrid scheme: (a) using the first guess of APR algorithm as the initialization; (b) carrying on the iteration with Multi-stage algorithm. Its flowchart is illustrated in Fig. 3. The symbol  $I_N$  denotes the measured intensity.  $G$  is the propagation operator, which represents the diffraction computation in free space. The superscript ‘ $\alpha$ ’ and ‘ $\alpha'$ ’ denote forth and back propagation separately.

In order to evaluate the convergence stability of three existing algorithms and the hybrid approach for the measurements from the whole diffraction field, we define a parameter, GPRQ (global phase retrieval quality).  $P_{Z_0,d}$  represents the reconstructed phase distribution under the first diffraction distance  $Z_0$  and the interval  $d$ . The variables  $(P_{Z_0,d}^1, P_{Z_0,d}^2, \dots, P_{Z_0,d}^{N_1+N_2})$  denote overall reconstructed results for whole diffraction field. In addition, we emphasize on whether or not phase retrieval is sufficiently convergent, in this case,  $\text{LSTD}(P_{Z_0,d})$  must be a negative parameter here. If its LSTD satisfies

$$\text{LSTD}(P_{Z_0,d}) > \frac{1}{\beta} \min \left[ \text{LSTD} \left( P_{Z_0,d}^1, P_{Z_0,d}^2, \dots, P_{Z_0,d}^{N_1+N_2} \right) \right], \quad (3a)$$

Download English Version:

<https://daneshyari.com/en/article/5007655>

Download Persian Version:

<https://daneshyari.com/article/5007655>

[Daneshyari.com](https://daneshyari.com)